ELECTRONIC SUPPLEMENTARY INFORMATION (ESI)

$Co_{3-x}Fe_xO_4$ Inverse Opals with Tunable Catalytic Activity for High-Performance Overall Water Splitting

Thi Hong Trang Nguyen[1,2], Zviadi Zarkua[1], Chinnabathini Vana Chinnappa[1], Wenjian Hu[1,3], Sreeprasanth Pulinthanathu Sree[4,5], Didier Grandjean[1], Deepak Pant[3], and Ewald Janssens[1,*]

[1] Quantum Solid-State Physics (QSP), Department of Physics and Astronomy, KU Leuven, Celestijnenlaan 200 D, 3001 Leuven, Belgium
[2] Faculty of Natural Sciences, Quy Nhon University, 170 An Duong Vuong, Quy Nhon, Binh Dinh, Vietnam
[3] Separation and Conversion Technology, Flemish Institute for Technological Research (VITO), Boeretang 200, 2400 Mol, Belgium
[4] Center for Surface Chemistry and Catalysis, KU Leuven, Celestijnenlaan 200 F, 3001 Leuven, Belgium
[5] Department of Materials Engineering, KU Leuven, 3001 Leuven, Belgium
* ewald.janssens@kuleuven.be

CONTENT

Figure S1 a) Pictures of solution-stabilized metal ions in ethanol, from left to right: Co, 2Co1Fe, 1Co1Fe, 1Co2Fe, and Fe. b) As-prepared mesoporous samples on nickel foam substrate, from left to right: Co, 2Co1Fe, 1Co1Fe, 1Co2Fe, and Fe.

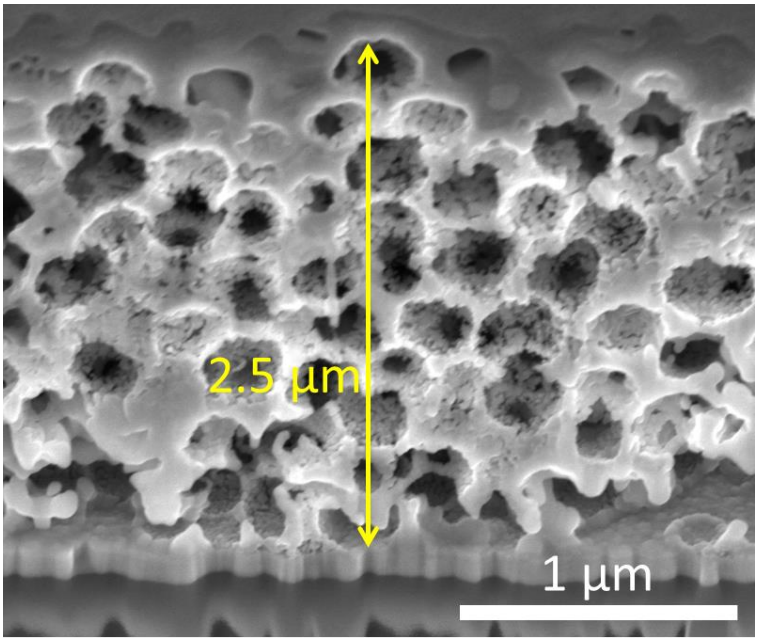

Figure S2 Cross-sectional SEM image of *m*-CFO with a precursor Fe:Co ratio of 1:1 reveal that the thickness of inverse opal thin film on the substrate of about 2.5 µm.

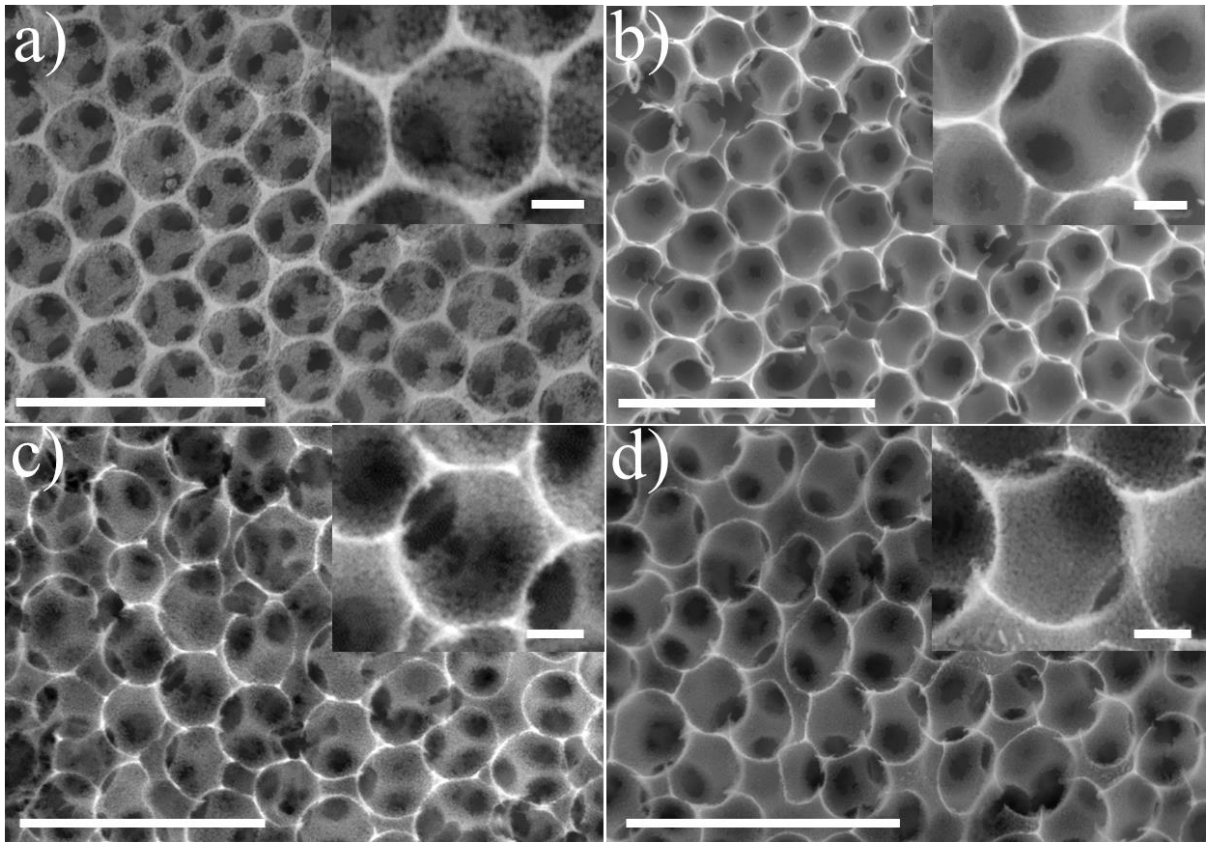

Figure S3 SEM images of the different m-CFO structures: a) Co, b) Fe, c) 2Co1Fe, and d) 1Co2Fe. Scale bars are 1 µm. The SEM images confirm the highly uniform coating layer of catalysts on the NF substrates. Insets are the corresponding high-resolution SEM images and have scale bars of 100 nm.

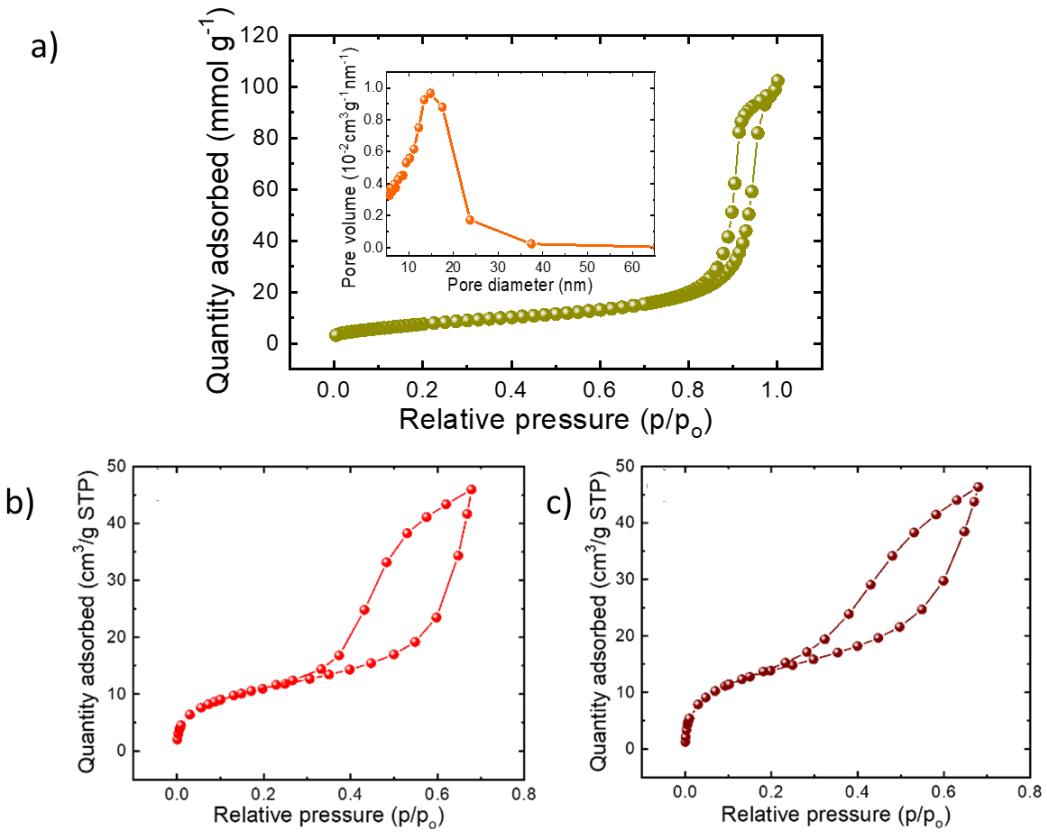

Figure S4 a) Nitrogen sorption isotherms and the pore size distributions (inset) for the 1Co1Fe sample. Krypton sorption isotherms for the b) 2Co1Fe and c) 1Co2Fe samples.

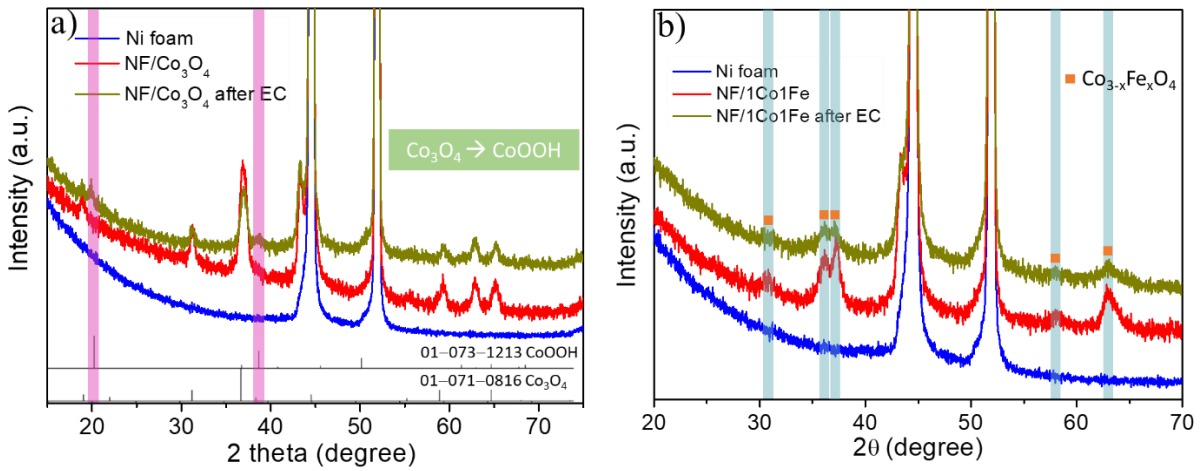

Figure S5 Comparison of XRD patterns of a) Co_3O_4 and b) 1Co1Fe samples on NF substrates before and after electrochemical (EC) reactions.

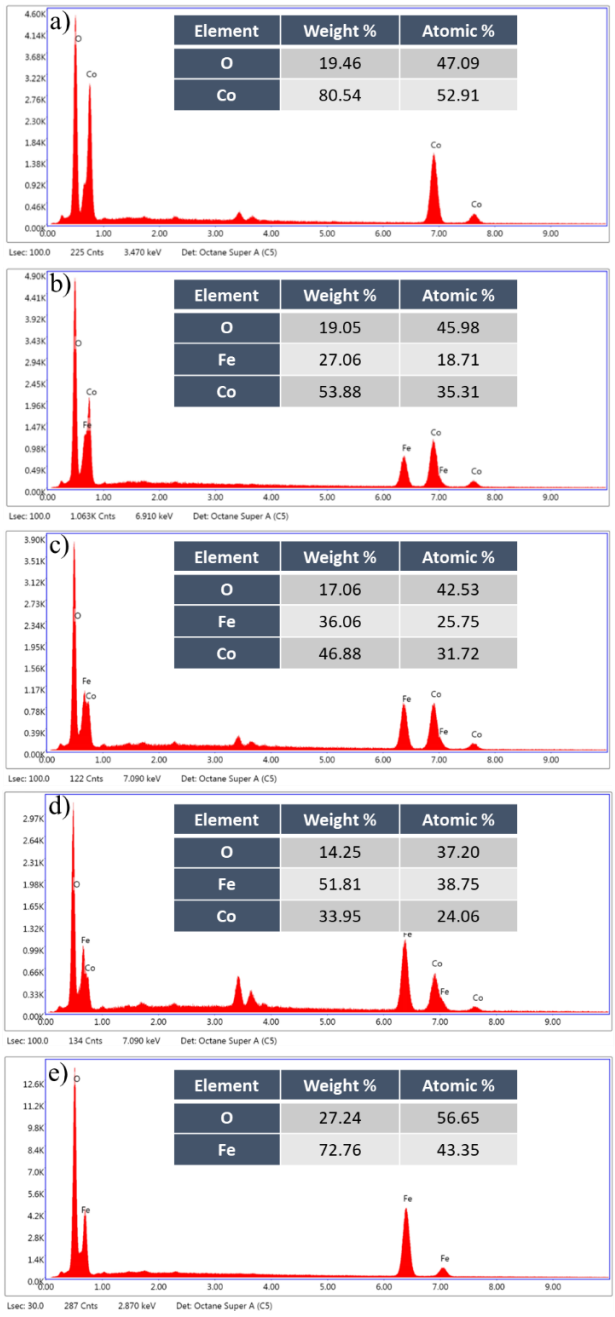

Figure S6 EDX patterns of the series of spinel catalysts: a) *m*-Co_3O_4, b) 2Co1Fe, c) 1Co1Fe, d) 1Co2Fe, and e) *m*-Fe_2O_3. The insets contain calculated percentages of the elements (see below) in the samples, both expressed as weight and atomic percentages.

The x values for different Co:Fe *m-CFOs*, i.e. $Co_{3-x}Fe_xO_4$, were extracted from the mass percentages of Fe, Co, and O as determined from EDX.

With the atomic mass of Co 58.93 g/mol, Fe 55.85 g/mol, and O 16.00 g/mol, the mass contributions of Co, Fe, and O in m-CFO are 58.93*(3-x) g/mol, 55.85*x g/mol, and 16.00*4 g/mol, respectively. The weight% were calculated as follows: Co: 58.93*(3-x)/(58.93*(3-x) + 55.85*x + 64.00)*100%, Fe: 55.85/(58.93*(3-x) + 55.85*x + 64.00)*100%, O: 64.00/(58.93*(3-x) + 55.85*x + 64.00)*100%.

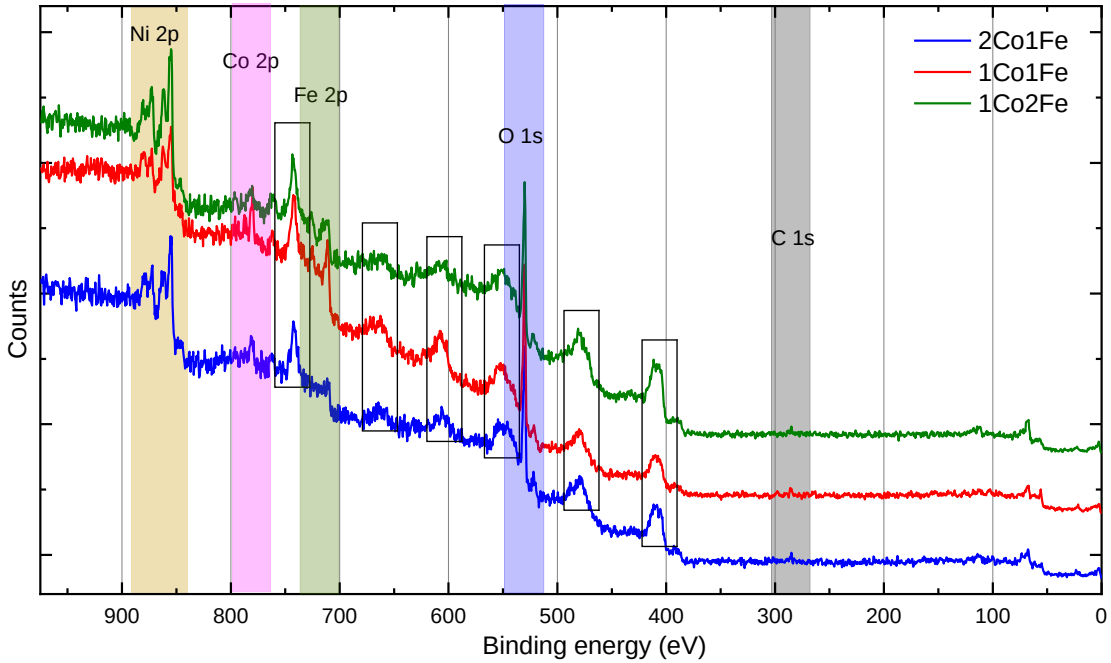

Figure S7 Wide-scan XPS spectra of the 2Co1Fe, 1Co1Fe, and 1Co2Fe m-CFO samples.

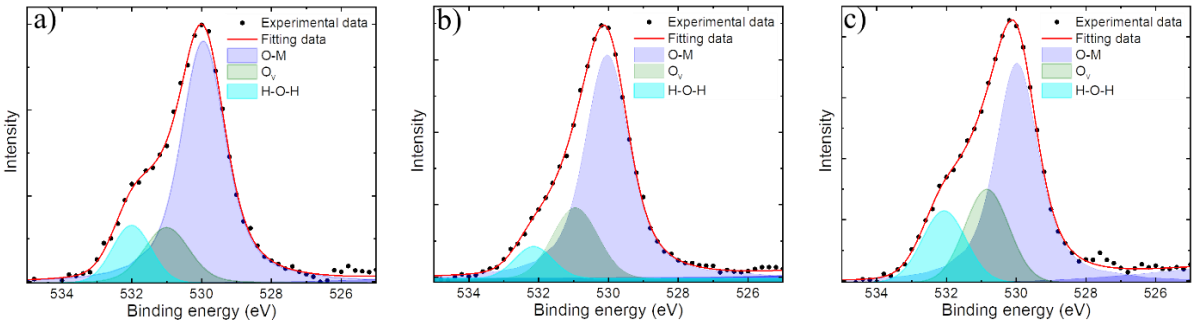

Figure S8 O 1s XPS spectra of (a) 2Co1Fe, (b) 1Co1Fe and (c) 1Co2Fe.

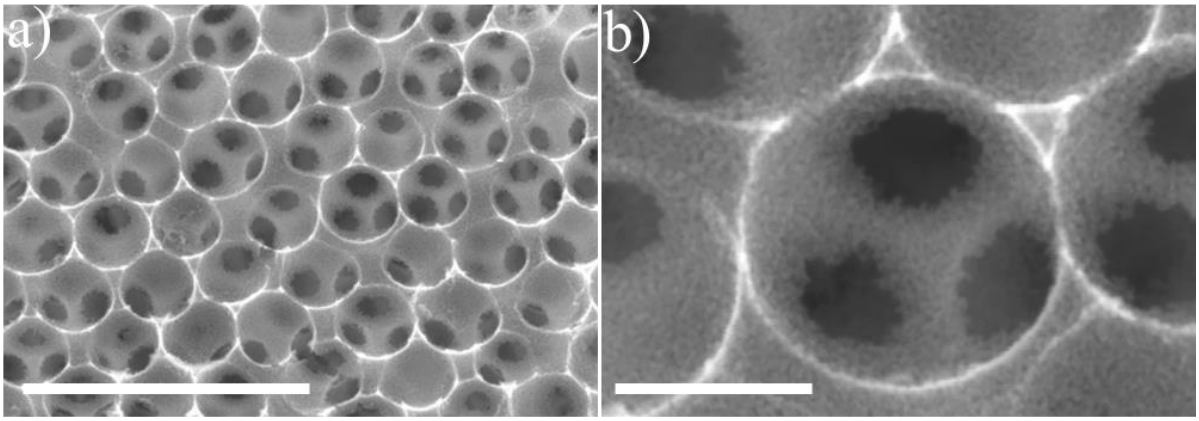

Figure S9 SEM images with different magnifications of 1Co1Fe after electrochemical reactions in 1M KOH. Scale bars: (a) 1 µm, (b) 200 nm.

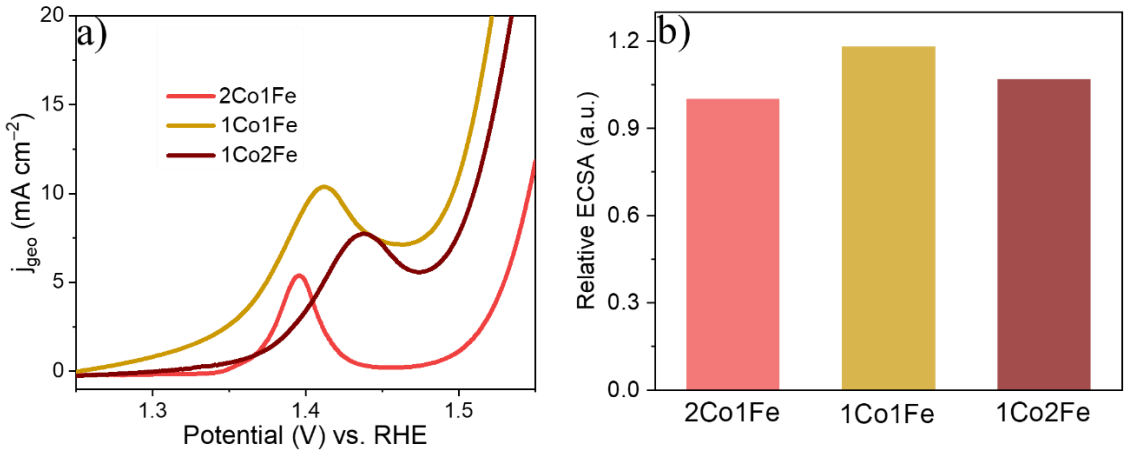

Figure S10 (a) LSVs showing the Co^{4+}/Co^{3+} formation peak used for area integration. (b) Relative electrochemical surface area (ECSA) of 2Co1Fe, 1Co1Fe, and 1Co2Fe catalytic interfaces in 1 M KOH. The ECSA of 2Co1Fe was set equal to one.

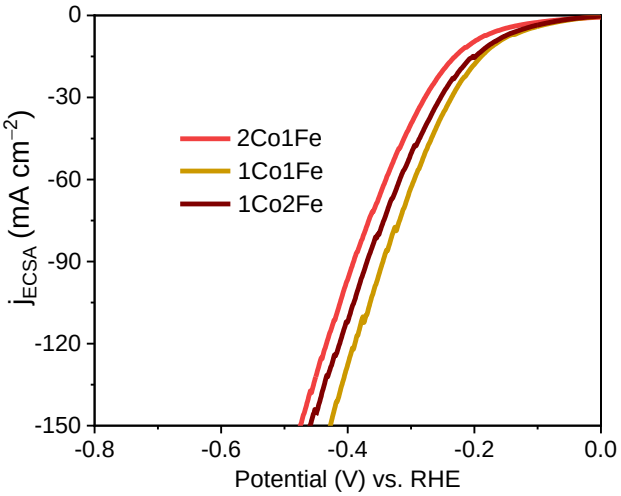

Figure S11 The relative ECSA-normalized LSVs for HER of the *m*-CFO IOs samples with different Co:Fe ratios.

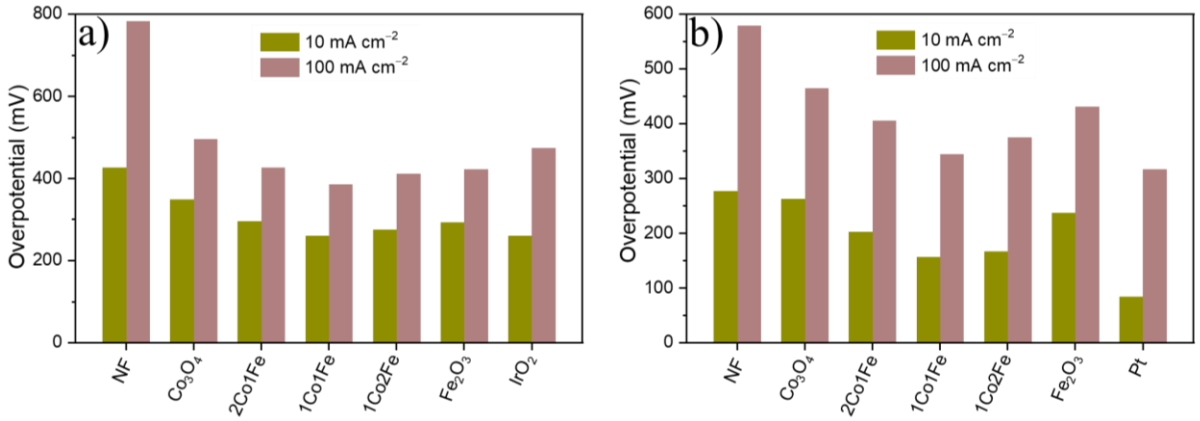

Figure S12 Comparison of overpotential values η_{10} and η_{100} for the different catalysts in the (a) OER and (b) HER processes.

Calculation of the oxygen deficiency

The amount of oxygen needed to form well-defined crystalline phases in $Co_{3-x}Fe_xO_4$, O_{need}, can be determined by assuming charge neutrality and considering the oxidation states of Fe and Co, $OS_{Fe,}$ and OS_{Co}, as obtained from the XPS measurements (columns 4 and 5 in Table 2).

$$O_{need} = ((3-x)\, OS_{Co} + x\, OS_{Fe})/2$$

The oxygen deficiency, $O_{def\%}$, is then calculated as the opposite of the difference between the amount of oxygen from the molecular formula, which was obtained from EDX and XRD data (column 4, Table 1, which equals 4), and O_{need}:

$$O_{def\%} = -(4 - O_{need}) / O_{need} \times 100\%.$$

Example for 1Co1Fe with molecular formula $Co_{1.5}Fe_{1.5}O_4$

$$O_{need} = (2.70 \times 1.5 + 3 \times 1.5)/2 = 4.275$$

$$O_{def\%} = -(-4 - 4.275)/4.275 \times 100\% = 6.4\%$$

Determination number of active sites involved in OER and turnover frequency

In an alkaline medium, the OER is often assumed to follow:[S1]

$$* + OH^- \leftrightarrow *OH + e^-$$

$$*OH + OH^- \leftrightarrow *O + H_2O + e^-$$

$$*O + OH^- \leftrightarrow *OOH + e^-$$

$$*OOH + OH^- \leftrightarrow * + O_2 + H_2O + e^-$$

In this case, three OER intermediates (*OH, *O, and *OOH) are adsorbed onto the active surface of the catalyst. Figure S10a shows the Co^{4+}/Co^{3+} peaks in the LSVs of the *m*-CFO IO electrodes. As the Fe content in $Co_{3-x}Fe_xO_4$ IO increases, the Co^{4+}/Co^{3+} wave shifts anodically. The shift is consistent with substitution of Fe in Co sites of CoO_x and $Co(OH)_2/CoOOH$. [S2],[S3] Laouini et al. added Fe to nanocrystalline Co_3O_4 films and observed a similar effect with an increased lattice constant, consistent with Fe incorporation into the nanocrystalline Co_3O_4.[S4] The Fe does not have any redox features in this potential range and remains nominally Fe^{3+}.[S5] Hence, it can be assumed that the number of Co^{3+} ions getting converted into Co^{4+} ions equals the number of active sites catalyzing the OER.

The integrated area of the Co^{4+}/Co^{3+} redox peak, and the corresponding charge associated with Co^{4+}/Co^{3+} formation, is proportional to the ECSA of *m*-CFO IO catalysts.[S6] From Figure S10a, the calculated areas for 2Co1Fe, 1Co1Fe, and 1Co2Fe are 1.75, 1.97, and 1.88×10^{-4} A V, respectively, corresponding to 21.9, 24.6, and 23.5×10^{16} active sites involved in the OER reaction, respectively (see below for calculation of the 2Co1Fe sample). These values are proportional to the ECSA.

Using the number of active sites, the relative ECSA was calculated by assuming that the number of active sites that are involved in OER with the 2Co1Fe sample exactly covers a geometrical area of 1 cm^2. Hence, the relative ECSA of 1Co1Fe and 1Co2Fe to that of 2Co1Fe are 1.18, and 1.07, respectively. The values are plotted in Figure S10b.

Example for 2Co1Fe:

- Area under redox peak: 1.75×10^{-4} A V
- Charge associated with redox peak (at scan rate of 0.005 V s^{-1}):
  1.75×10^{-4} A V / 0.005 V s^{-1} = 35.1×10^{-3} C
- Number of electrons transferred = 35.1×10^{-3} C / 1.602×10^{-19} C = 21.9×10^{16}

  Since the Co^{4+}/Co^{3+} formation reaction is a single electron transfer reaction, the number of electrons transferred during the reaction equals the number of active sites involved in the reaction is 21.9×10^{16}.

- Turnover frequency at 1.6 V vs. RHE:
  TOF = 46.5 mA/cm^2 × 6.023×10^{23}/ (4 × 96485 C × 21.9×10^{16} cm^{-2}) = 0.33 s^{-1}

References

[S1] N. T. Suen, S. F. Hung, Q. Quan, N. Zhang, Y. J. Xu, H. M. Chen, Electrocatalysis for the Oxygen Evolution Reaction: Recent Development and Future Perspectives. *Chem. Soc. Rev.*, 2017, **46**, 337–365.

[S2] R.D.L. Smith, M.S. Prévot, R. D. Fagan, S. Trudel, C. P. Berlinguette, Water Oxidation Catalysis: Electrocatalytic Response to Metal Stoichiometry in Amorphous Metal Oxide Films Containing Iron, Cobalt, and Nickel. *J. Am. Chem. Soc.*, 2013, **135**, 11580–11586.

[S3] M. S. Burke, M. G. Kast, L. Trotochaud, A. M. Smith, S. W. Boettcher, Cobalt–Iron (Oxy)Hydroxide Oxygen Evolution Electrocatalysts: The Role of Structure and Composition on Activity, Stability, and Mechanism. *J. Am. Chem. Soc.*, 2015, **137**, 3638–3648.

[S4] E. Laouini, M. Hamdani, M. I. S. Pereira, J. Douch, M. H. Mendonça, Y. Berghoute, R. N. Singh, Preparation and Electrochemical Characterization of Spinel Type Fe–Co_3O_4 Thin Film Electrodes in Alkaline Medium. *Int. J. Hydrogen Energy*, 2008, **33**, 4936–4944.

[S5] M. E. G. Lyons, M. P. Brandon, Redox Switching and Oxygen Evolution Electrocatalysis in Polymeric Iron Oxyhydroxide Films. *Phys. Chem. Chem. Phys.*, 2009, **11**, 2203–2217.

[S6] S. Anantharaj, S. Kundu, Do the Evaluation Parameters Reflect Intrinsic Activity of Electrocatalysts in Electrochemical Water Splitting? *ACS Energy Lett.*, 2019, **4**, 1260–1264.